Received: 27 July 2020 | Revised: 1 February 2021 | Accepted: 28 February 2021

DOI: 10.1002/ep.13634

REMEDIATION TREATMENT

ENVIRONMENTAL PROGRESS & SUSTAINABLE ENERGY

Assessment of lead biosorption performance of spent *Gelidiella acerosa* (marine macro algae): Optimization, isotherm, kinetic, and column studies

John Babu D

Department of Biotechnology, Vignan's Foundation for Science, Technology, and Research, Guntur, Andhra Pradesh, India

Correspondence
D. John Babu, Department of Biotechnology, Vignan's Foundation for Science, Technology, and Research, Vadlamudi, Guntur, 522213, Andhra Pradesh, India.
Email: johnbabud77@gmail.com

Abstract

In this research, biosorption of Lead using spent *Gelidiella acerosa* from synthetic aqueous phase was studied in batch and fixed bed modes. Biosorbent was prepared from waste biomass of *Gelidiella acerosa* after extraction of agar as a model industrial waste recycle. The process efficiency and optimum lead uptake were evaluated by considering initial pH, lead concentration, and biosorbent dosage as process variables and contact time and temperature as fixed parameters. Central composite design of Response Surface Methodology was used to optimize process parameters and ANOVA showed that initial pH of lead solution significantly influences the biosorption. Interaction effects of different process parameters on process efficiency were analyzed with the help of surface response plots. The highest lead biosorption of 90.75% was noticed at optimum conditions of pH 5.15, initial lead concentration 27.35 mg L^{-1} and biosorbent dosage 0.04 g. Various kinetic equations were used to analyze the biosorption mechanism and found that metal binding is due to chemical reaction with multi stage mass transfer. Langmuir isotherm was found to be well fitted to equilibrium data. Column studies were also conducted to assess the suitability of the process to continuous operations. The most popular Thomas and Yoon nelson models were used to evaluate the fitness of column studies. Biosorbent was characterized using FTIR and SEM to determine surface functional groups and surface texture.

KEYWORDS
fixed bed, kinetics, lead, optimization, spent *G. acerosa*

1 | INTRODUCTION

Contamination of the aqueous environment with the infusion of heavy metal ions from industrial discharges became a severe global problem. Heavy metals have been top investigated since their existence in the environment due to their long-term persistence, bioaccumulation in the food chain, and toxicity even at low concentrations.[1-3] Moreover, many reports of literature highlighted that some heavy metals are potential carcinogens even at low concentrations[4,5] and some will accumulate in various tissues and causes gastric infections, mutagenicity, and mental disorders.[2,6]

Among heavy metals, Lead (Pb[II]) has got greatest attention due to its high toxicity and ruinous effects on humans and wildlife. The main sources that discharges Pb(II) into water streams include various industrial wastewater such as battery industries, automobiles, paints, fertilizer, metal plating and finishing, electronic, combustion fossil fuel, etc.[7] Humans exposure to Pb(II) affects nerves, digestion, urinary, reproductive and developmental, cardiovascular, endocrine, immune, bone, and other organ systems.[8] More serious is that Pb(II) affects the growth and mental development of infants and young children, impairs brain function such as cognition.[9] Hence, elimination of traces of Pb(II) from industrial waste effluents before discharging into water streams is essential.

In wastewater treatment, various physicochemical and electrochemical methods such as filtration, electrostatic precipitation, coagulation-sedimentation, and ion exchange were used for the removal of toxic metals.[10-12] These methods were deemed as ineffective at low concentrations, expensive, and generate toxic secondary sludge.[13,14] Numerous researchers focused their attention on introducing new alternatives to these technologies which are more eco-friendly and low cost, which can be successfully applied at large scale in wastewater treatment plants.[15-17] It has been proven that biosorption and bioaccumulation which uses the natural capacity of plants and/or microorganisms to remove heavy metals can be efficiently applied for heavy metals removal even at lower concentrations.[18,19]

Algae a renewable and naturally abundantly available biomass was well reported by researchers as biosorbent for wastewater treatment.[20] Some marine and fresh water algae showed higher biosorption potential (biosorption of Au, Ag, and Co) than synthetic adsorbents like activated carbon, nano-fibers and ion-exchange membranes.[21] It was also reported that in case of highly toxic metals the uptake capacities of brown algae are higher than other algae (green and red algae).[22] Hence, marine brown algae *Gelidilla acerosa* (*G. acerosa*) was selected as biosorbent for this study. The novelty of the present study is using waste product of agar extraction process as an adsorbent for removal of lead from industrial wastewater.

The main intents of the this study are (a) to study the Pb(II) sorption potential of spent *G. acerosa* from aqueous medium, (b) to optimize influential process parameters such as initial pH of Pb(II) solution, initial Pb(II) concentration, and biosorbent dose to attain maximum biosorption using Response Surface Methodology (RSM) (c) to determine the process parameters for fixed bed column studies to assess the suitability of process for industrial scale continuous operations.

2 | MATERIALS AND METHODS

2.1 | Reagents and biosorbent

The equivalent amount of $Pb(NO_3)_2$ was dissolved in 1 L double distilled water to obtain 1000 PPM stock solution and working samples of Pb(II) were prepared from stock solution by making accurate dilutions for each batch experiment. All reagents utilized in experiments were of analytical grade. Brown marine macro algae (*G. acerosa*) was obtained from the coast of Gulf of manar, India. Collected plants were washed several times with normal and distilled water.[23] Agar extraction was carried out by following the protocol described by Dulla et al.[24] The waste biomass after agar extraction was filtered, sundried, grounded, and sieved using standard mesh. The prepared biosorbent was directly used without any further treatment.

2.2 | Biosorption experiments

To determine the equilibrium contact time, experiments were conducted by taking 50 ml of working samples of 50 mg L^{-1} concentration at pH of 5 by adding 0.01 g of spent *G. acerosa* in an Erlenmeyer flask, and agitated at speed of 120 rpm for different contact times up to 120 min. After filtration, the filtrate was analyzed for remaining Pb(II) using Atomic Adsorption Spectroscopy.[25] The Pb(II) uptake was calculated using the below equation[26]:

$$q_e = \frac{V(C_o - C_f)}{1000m} \quad (1)$$

where C_0 and C_f (mg L^{-1}) are the initial and equilibrium Pb(II) concentrations, q_e is Pb(II) uptake (mg g^{-1}), V is working sample volume (ml), and m is weight of biosorbent (g). The same data was used for kinetic analysis. For optimization studies, experiments were conducted by following the experimental design matrix of RSM.[27] All experiments were conducted by taking 50 ml of sample solution in Erlenmeyer flask and agitated at 120 rpm for 100 min (predetermined contact time). Equilibrium studies data was generated by conducting experiments with variable initial Pb(II) concentration from 20 to 100 mg L^{-1} with an interval of 20 mg L^{-1} and other parameters were maintained at optimum values (after optimization). In order to determine the thermodynamic feasibility of biosorption, thermodynamic parameters such as ΔG, ΔH, and ΔS were calculated by conducting biosorption experiments at three temperatures, ie, 303, 313, and 323 K.

2.3 | Optimization

RSM was adopted to predict the optimum process parameters and also to establish interaction effects of selected three process parameters such as the initial pH of the solution, initial pollutant concentration and biosorbent dosage on the performance of spent *G. acerosa*. The limits of the selected parameters were summarized in Table 1 and the model equation developed by RSM is given below.[28]

$$y = \alpha_0 + \sum_{i=1}^{n} \alpha_i x_i + \sum_{i=1}^{n} \alpha_{ij} x_i x_j + \sum_{i=1}^{n} \alpha_{ii} x_i^2 \quad (2)$$

where y is percent biosorption of Pb(II); α_0 is offset value; x is variable; α_i, α_{ii}, and α_{ij} are coefficients of first order, second order, and interaction terms, respectively; n is number of parameters. The experiments were designed using central composite design of RSM and the results were validated with quadratic model. The design matrix, experimental results and model predicted values were summarized in Table 2.

TABLE 1 The ranges of input variables for optimization of Pb(II)

S. No.	Input variable	Range
1	Initial pH of Pb(II) solution (x_1)	3-7
2	Initial Pb(II) concentration (x_2)	20-100 mg L^{-1}
3	Biosorbent dosage (x_3)	0.01-0.05 g

TABLE 2 Design matrix and experimental and predicted responses for biosorption of Pb(II)

Standard order	Initial pH of Pb(II) solution	Initial Pb(II) concentration	Biosorbent dosage	Experimental % biosorption	Predicted % biosorption
1	3.00	20.00	0.01	46.01	46.38
2	7.00	20.00	0.01	50.71	51.08
3	3.00	100.00	0.01	38.15	38.32
4	7.00	100.00	0.01	41.46	41.63
5	3.00	20.00	0.05	56.4	56.77
6	7.00	20.00	0.05	60.48	60.85
7	3.00	100.00	0.05	48.03	48.20
8	7.00	100.00	0.05	50.72	50.89
9	3.00	60.00	0.03	58.39	57.33
10	7.00	60.00	0.03	62.09	61.02
11	5.00	20.00	0.03	90.01	88.54
12	5.00	100.00	0.03	80.2	79.53
13	5.00	60.00	0.01	79.25	78.18
14	5.00	60.00	0.05	89.07	88.01
15	5.00	60.00	0.03	87.66	88.52
16	5.00	60.00	0.03	88.43	88.52
17	5.00	60.00	0.03	88.04	88.52
18	5.00	60.00	0.03	87.54	88.52
19	5.00	60.00	0.03	86.57	88.52
20	5.00	60.00	0.03	88.64	88.52

2.4 | Column biosorption study

The fixed bed column experiments were carried out with a cylindrical Plexiglass column of 1.5 cm ID and 30 cm height. The solution was passed through the bed using peristaltic pump (PP-20-EX, Miclins, India).[29] The schematic representation of fixed bed is shown in Figure 1. The column was initially run with distilled water to ensure pollutant free bed, later it was run with lead solution of two concentrations, ie, 50 and 100 mg L^{-1} to determine the performance of fixed bed and to model the continuous column studies. The column studies were conducted at room temperature and initial pH of 5.13.

The mass of the total Pb(II) that was introduced into the column (m_t) was determined by the following equation.[30]

$$m_t = \frac{C_0 F t_t}{1000} \tag{3}$$

The mass of the Pb(II) adsorbed onto the biosorbent during column experiment (q_t) was evaluated using the following equation.[31]

$$q_t = \frac{C_0 F}{1000} X \left(t_t - \int_{t=0}^{t=t_t} \frac{C_t}{C_0} dt \right) \tag{4}$$

The percent biosorption of Pb(II) in column experiments ($Y(\%)$) was calculated by the expression given below.[32]

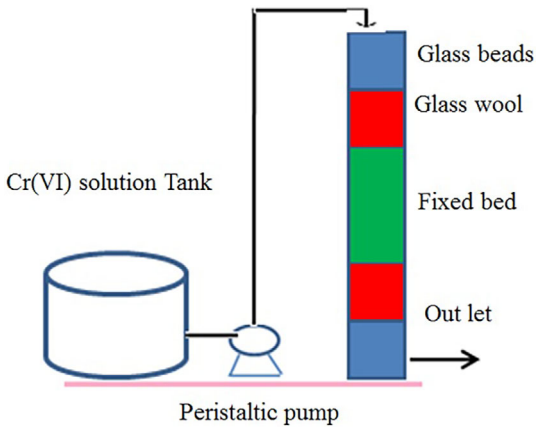

FIGURE 1 Schematic representation of fixed bed column operation [Color figure can be viewed at wileyonlinelibrary.com]

$$Y(\%) = \frac{q_t}{m_t} X100 \tag{5}$$

And the maximum biosorption potential of Pb(II) in column studies (q_e) was determined using the following equation.[33]

$$q_e = \frac{q_t}{W} \tag{6}$$

where C_0 is initial Pb(II) concentration in mg L^{-1}, C_t is final concentration of Pb(II) at time t in mg L^{-1}, F is the flow rate in ml h^{-1}, t_t is biosorbent saturation time, and W is weight of biosorbent.

2.5 | Desorption studies

To regenerate the biosorbent, desorption experiments were performed in batch system using 0.1 M HNO_3 as eluent.[25] The regeneration capacity of biosorbent was assessed in four biosorption-desorption cycles. In each desorption experiment, 0.01 g of metal loaded biomass was eluted with 50 ml 0.1 M HNO_3. The efficiency of desorption was calculated as percentage of Pb(II) desorbed from the initially biosorbed Pb(II) mass. The percent desorption of Pb(II) was calculated from the ratio of metal desorbed to metal adsorbed.

2.6 | Biosorbent characterization and zero-point charge

The surface structure and morphological features of biosorbent before and after Pb(II) removal were studied using SEM (Tescan Mira 3 XMU) and FTIR (Bruker Tensor II). The zero-point charge (pH_{pzc}) is used to ascertain the influence of pH on metal uptake. The pH_{pzc} of spent *G. acerosa* was determined by following the protocol of Ferro-García et al.[34] According to the protocol, 30 ml of 0.01 M NaCl was taken in Erlenmeyer flasks and 1 g spent *G. acerosa* was added to each flask by adjusting the solution pH in the range of 3–9. The solution pH was altered using 0.1 M NaOH/HCl solutions.[35] The solutions were agitated for 24 h and the end pH of the solutions was noted. A plot was drawn between pH_{in} vs ΔpH and the intercept of plot was considered as pH_{pzc} of spent *G. acerosa*.

3 | RESULT AND DISCUSSION

3.1 | Batch study

3.1.1 | Optimization of biosorption parameters

The time reliance of biosorption of Pb(II) at initial concentration of 50 mg L^{-1} was illustrated in Figure 2A. It was noticed that at the initial

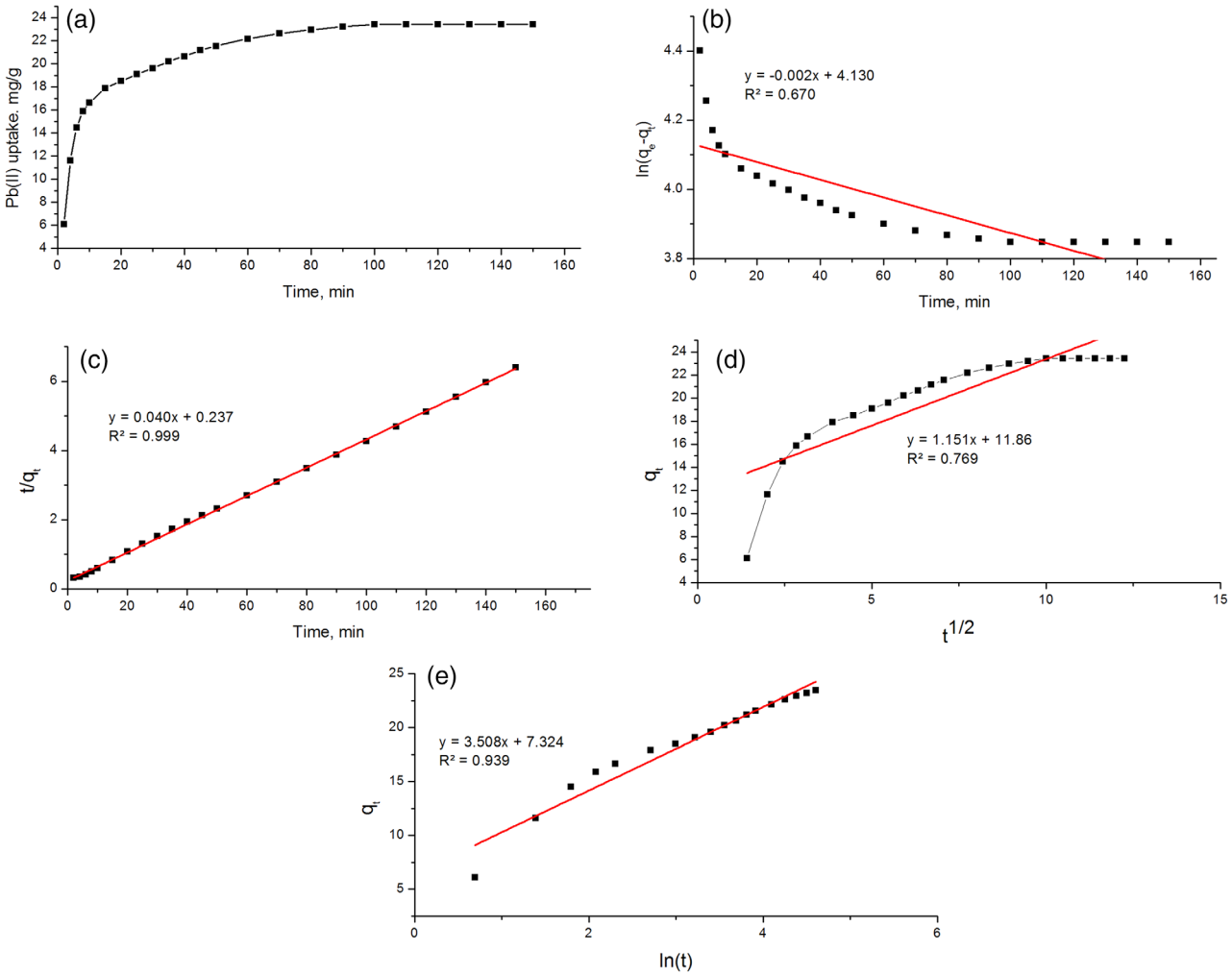

FIGURE 2 Effect of contact time and kinetic models for biosorption of Pb(II) (a). Effect of contact time on Pb(II) uptake (b). Pseudo-first order kinetics (c). Pseudo-second order kinetics (d). Weber Morris model (e). Elovich model for Pb(II) uptake [Color figure can be viewed at wileyonlinelibrary.com]

stage of biosorption the metal removal rates were very high and almost 70% Pb(II) was taken up within first 30 min of the process. Further, though the removal rates were decreased, metal removal was increased and attained saturation after 100 min. Hence, 100 min were fixed as equilibrium contact time for maximum uptake of Pb(II) onto spent *G. acerosa*. Quite high adsorption rates at initial minutes are better explained due to availability of large number of fresh and active pores on the surface and sufficient number of metal ions in solution. Hence, rapid film diffusion onto biosorbent surface followed by quick pore diffusion into intra particle matrix contributed rapid equilibrium.[36] Further, gradual decrease in Pb(II) removal was because of reduction and occupancy of active sites. Regti et al.[37] reported similar results for Pb(II) biosorption using *Persea americana*-activated carbon.

After fixing the contact time, the optimum values of other process variables were determined using RSM of Design Expert. Table 1 shows the ranges of parameters selected for optimization and Table 2 shows the design matrix of experimental tests obtained from RSM, including the experimental and predicted responses. The ANOVA was used to evaluate RSM results and summarized in Table 3. Very high calculated F value (Fcal = 576.32) and very low *P* value (<.0001) demonstrating the competency of model. The result also reveals that all the three parameters are effective individually; however, the interaction terms are having higher values of probability and are considered as insignificant. The model equation representing the biosorption of Pb(II) in terms of effective parameters is given as:

$$\%\text{Biosorption of Pb(II)} = 88.52 + 1.85x_1 - 4.51x_2 + 4.91x_3 - 0.35x_1x_2 - 0.15x_1x_3 - 0.13x_2x_3 - 29.35x_1^2 - 4.48x_2^2 - 5.43x_3^2 \quad (7)$$

In the above equation x_1 and x_3 (pH of Pb(II) solution and biosorbent dosage) are having positive coefficients indicating that these variables have positive (increasing) effect on Pb(II) removal, whereas x_2 (initial Pb(II) concentration) is having negative coefficient indicating negative effect (decreasing) effect on Pb(II) removal. The similar results were demonstrated by Mousavi et al.[38] for removal of lead onto mixed culture of algal biomass and Babu et al.[39] for copper removal using sea urchin test.

The interaction effect plots were illustrated in Figure 3. From Figure 3A it can be perceived that initial pH of Pb(II) solution is the highest dominant parameter among others. The pH of solution significantly affects the ionic state of the solute and surface charge of biosorbent.[40] The efficiency of biosorbent increased along with pH up to 5, attained peak around 5.1 and then decreased. Variations in Pb(II) removal with initial pH of Pb(II) solution can be better explained with the surface charge variations of biosorbent. At low initial pH of the solution, due to protonation the surface of the biosorbent obtains positive charge. Therefore, at lower pH, because of repulsion between lead cations and positive surface charge the metal removal rates are very low. With the increasing pH, the number of sites with negative charge increases on biosorbent surface due to deprotonation. Hence, the metal removal efficiency increases with increase in pH of the solution.[41] The pH_{pzc} is a notable factor to explain variations in adsorptive potential of a surface. As shown in Figure 4, the pH_{pzc} of spent *G. acerosa* is 3.6. When pH of the solution <3.6, the positive surface charge of biosorbent repels the lead cations and consequently low metal removal rates registered. Whereas at pH > 3.6, the negative surface charge of biosorbent contributes for the increase in metal removal rates.

Figure 3(b) clearly shows interaction effect of initial pH of Pb(II) solution and biosorbent dosage on Pb(II) removal. It can be observed that the effect of biosorbent dosage is moderate, whereas pH of Pb(II) solution is extensive. Though there is increase in number of sites with increase of biosorbent dosage, the surface charge of active sites is remarkable in metal removal.[42] Figure 3(c) shows that the interaction effect of initial Pb(II) concentration and biosorbent dosage on Pb(II) removal. It can be observed that the effect of biosorbent dosage is

TABLE 3 ANOVA for optimization of Pb(II)

Source of variation	Sum of squares	df	Mean square	*F* value	*P* value Prob > *F*	
Model	6926.15	9	769.57	567.32	<.0001	Significant
A-Initial pH of Pb(II) solution (x_1)	34.15	1	34.15	25.18	.0005	
B-Initial Pb(II) concntration (x_2)	202.95	1	202.95	149.61	<.0001	
C-*G. acerosa* dosage (x_3)	241.28	1	241.28	177.87	<.0001	
x_1x_2	0.97	1	0.97	0.71	.4185	
x_1x_3	0.19	1	0.19	0.14	.7145	
x_2x_3	0.13	1	0.13	0.096	.7632	
x_1^2	2368.77	1	2368.77	1746.22	<.0001	
x_2^2	55.29	1	55.29	40.76	<.0001	
x_3^2	81.06	1	81.06	59.75	<.0001	
Residual	13.57	10	1.36			
Lack of fit	10.81	5	2.16	3.92	.0802	Not significant
Pure error	2.76	5	0.55			
Cor total	6939.71	19				

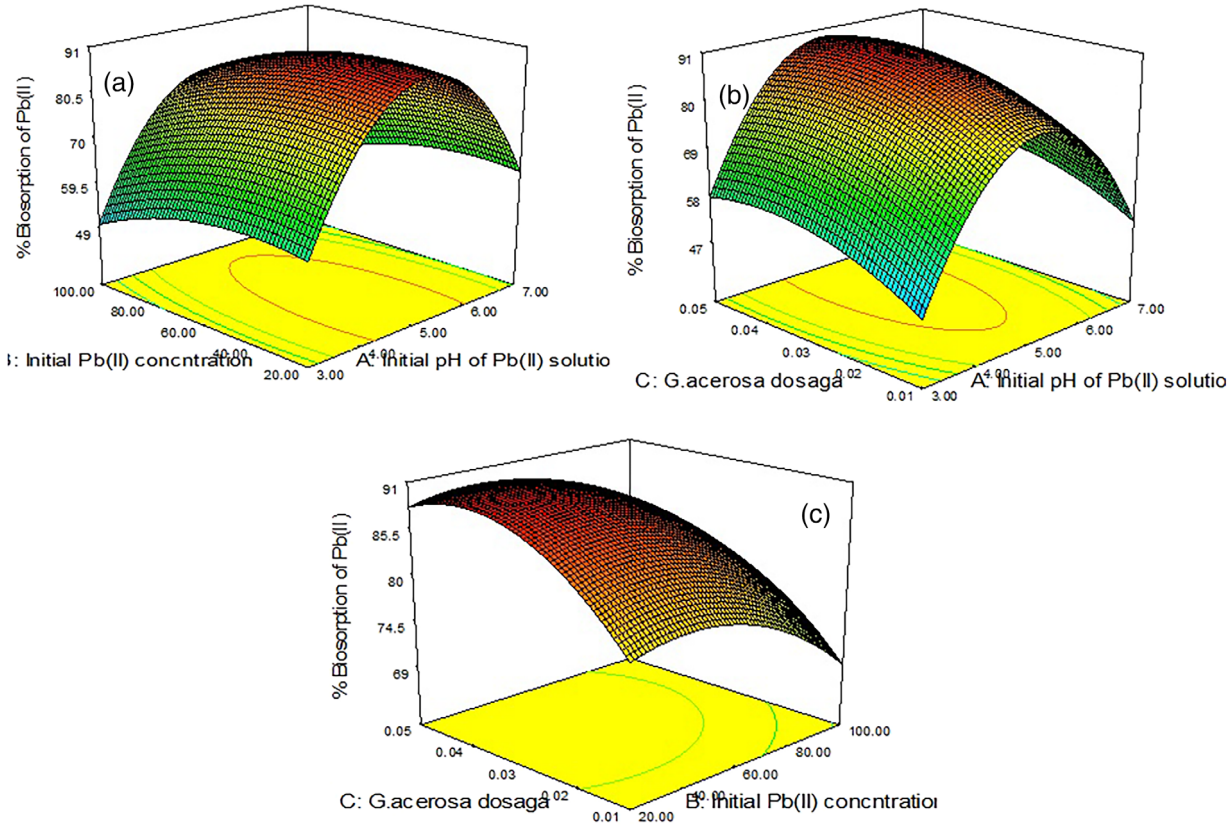

FIGURE 3 Effects of process parameters on biosorption potential of spent *G. acerosa* (a). Interaction effect of initial Pb(II) concentration and initial pH on biosorption of Pb(II) (b). Interaction effect of G.acerosa dosage and initial pH on biosorption of Pb(II) (c). Interaction effect of *G. acerosa* dosage and initial Pb(II) concentration on biosorption of Pb(II) [Color figure can be viewed at wileyonlinelibrary.com]

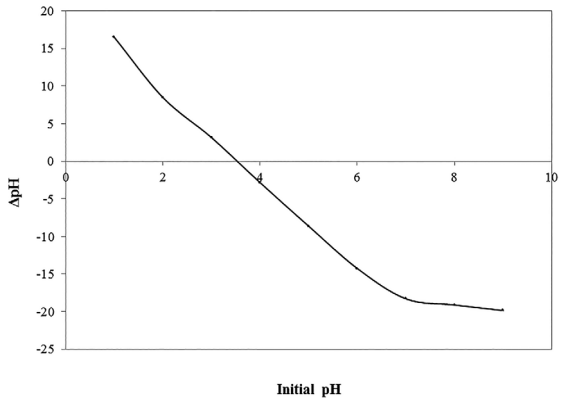

FIGURE 4 Point zero charge of spent *G. acerosa*

moderate, whereas initial Pb(II) concentration is significant. Though there are sufficient metal ions in solution, the number of active sites with attractive surface charge is essential for metal removal. In overall the interactive effect of initial pH of Pb(II) solution and biosorbent dosage had significant effect on Pb(II) removal

After developing empirical equation for Pb(II) removal, optimization of RSM was exploited to asses maximum Pb(II) uptake by *spent G. acerosa* and to determine optimum process parameters (Figure 5). The highest Pb(II) removal determined from RSM is 90.75% (Figure 3) at optimum process parameters of initial pH of Pb(II) solution 5.15, initial Pb(II) concentration of 37.35 mg L^{-1} and biosorbent dosage of 0.04 g. A fresh experiment was conducted at RSM predicted optimum process parameters and obtained 90% of Pb(II) removal which is approximately matching with the predicted value. Hence, the numerical values of process parameters at highest Pb(II) removal attained by RSM were noted as optimum process parameters for biosorption of Pb(II) onto *G. acerosa*.

3.1.2 | Kinetics

The kinetic constants are very important parameters in determining significant reaction mechanism, modeling and design of industrial scale biosorption process. Kinetic constants are also used in determining significant rate controlling step and nature of adsorption occurring in metal uptake. Psuedo-first, second order, Weber-Morris, and Elovich models were used to determine kinetic constants and the results were shown in Table 4. The current findings disclosed that second order equation was most competent model with high regression coefficient (R^2 = 0.999). It demonstrates that the mechanism behind metal binding is chemical reaction between solute and functional groups on biosorbent surface.[43] Moreover, fitness of kinetic data to Elovich model also confirms chemisorption. Further to investigate the

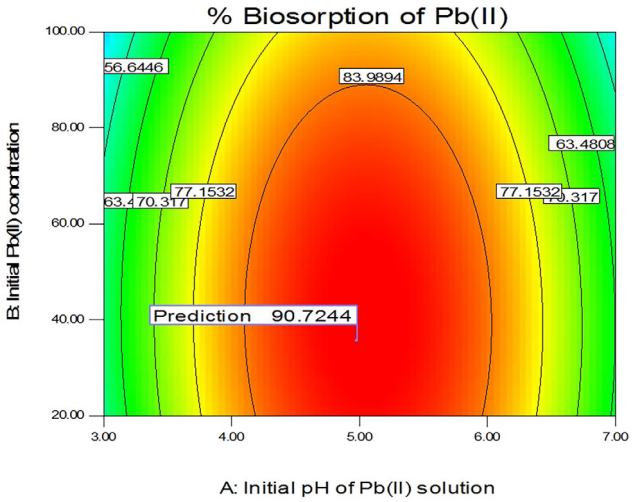

FIGURE 5 Optimization of biosorption of Pb(II) [Color figure can be viewed at wileyonlinelibrary.com]

TABLE 4 Kinetic models for biosorption of Pb(II)

1	Pseudo-first order model $\log(q_e - q_t) = \log q_e - k_1 t$	k_1	0.002 (min^{-1})
		q_e(exp)	23.44 mg g^{-1}
		q_e (cal)	17.5 mg g^{-1}
		R^2	0.67
2	Pseudo-second order model $\frac{t}{q_t} = \left(\frac{1}{k_2 q_e^2}\right) + \left(\frac{t}{q_e}\right)$	k_2	0.0067 mg (g min)$^{-1}$
		q_e(exp)	23.44 mg g^{-1}
		q_e (cal)	25 mg g^{-1}
		R^2	0.999
3	Weber Morris model $q_t = k_{id} t^{1/2} + C$	K_D	1.152 mg (g min ^{½})$^{-1}$
		C	11.86
		R^2	0.76
4	Elovich model $q_t = \beta \ln\alpha + \beta \ln t$	α	4.22 mg (g min)$^{-1}$
		β	3.508 g mg^{-1}
		R^2	0.93

rate controlling mechanism Weber-Morris model was implemented and found that (R^2 = 0.769) removal of Pb(II) alone does not explained by intra-particle diffusion model.[44] As shown in Figure 2(e), the plot is not linear for the total time of biosorption and can be split into two distinct phases which ascertains the two stages of biosorption. Moreover, the plot is not passing through origin which demonstrates that along with intra-particle diffusion, film diffusion also occurred during biosorption.[45] Hence, at the beginning Pb(II) ions were transferred from bulk medium onto the surface of spent *G. acerosa* through film diffusion. Later, Pb(II) ions were migrated into the spent *G. acerosa* by intra-particle transfer through pores.

3.1.3 | Equilibrium studies

Langmuir, Freundlich and Temkin equilibrium isotherms were employed to investigate more on Pb(II) biosorption potential of spent *G. acerosa* and the results were depicted in Figure 6 and summarized in Table 5. The results revealed that out of three models Langmuir is best fitted to equilibrium data with greatest R^2 of 0.999. It indicates that biosorption of Pb(II) onto spent *G. acerosa* was formation of monolayer on the homogenous surface. The theoretical maximum Pb(II) uptake calculated from Langmuir model is 27.02 mg g^{-1}. The current findings demonstrated that spent *G. acerosa* had significant biosorption capacity due to the presence of various functional groups on cell wall, thus it can be employed as an successful biosorbent without any further treatment in Pb(II) removal from industrial wastewater. Moreover spent *G. acerosa* showed higher biosorption capacity when compared to many other adsorbents reported in earlier studies as shown in Table 6.

3.1.4 | Biosorption thermodynamics

The thermodynamic energy functions for biosorption of Pb(II) onto spent *G. acerosa*, were determined using the following equations.[23]

$$K_D = \frac{q_e}{c_e} \tag{8}$$

$$\Delta G^0 = -RT\ln(K_D) \tag{9}$$

$$\ln(K_D) = \frac{\Delta S^0}{R} - \frac{\Delta H^0}{RT} \tag{10}$$

The ΔH^0 and ΔS^0 values were calculated from the slope and intercept of the plot of ln K_D vs 1/T, shown in Figure 7 and calculated values were provided in Table 7.

The decreasing negative values for ΔG^0 were found with increasing temperature. The negative values of change in Gibb's free energy indicates the spontaneous nature of Pb(II) biosorption onto spent *G. acerosa*. Further, the positive value of ΔH reveals the endothermic nature of biosorption of Pb(II) onto spent *G. acerosa*. Increase in temperature normally enhances biosorption because of increase in kinetic energy of solute molecules.[51] Moreover, the positive value of ΔS demonstrates the increased randomness at the solid/solution interface during the Pb(II) biosorption onto *G. acerosa*.

3.2 | Column studies

3.2.1 | Breakthrough curves

To assess the Pb(II) biosorption performance of *G. acerosa* in continuous mode operations and also to determine the dynamic parameters of biosorption process, fixed bed column studies were conducted at optimum process parameters and the resultant data were used to plot breakthrough curves (Figure 8). Column studies were carried out for two Pb(II) concentrations such as 50 and 100 mg L^{-1} at a flow rate of 5 ml/min by choosing other parameters at optimum values obtained from RSM. The results of breakthrough curves showed in Figure 8,

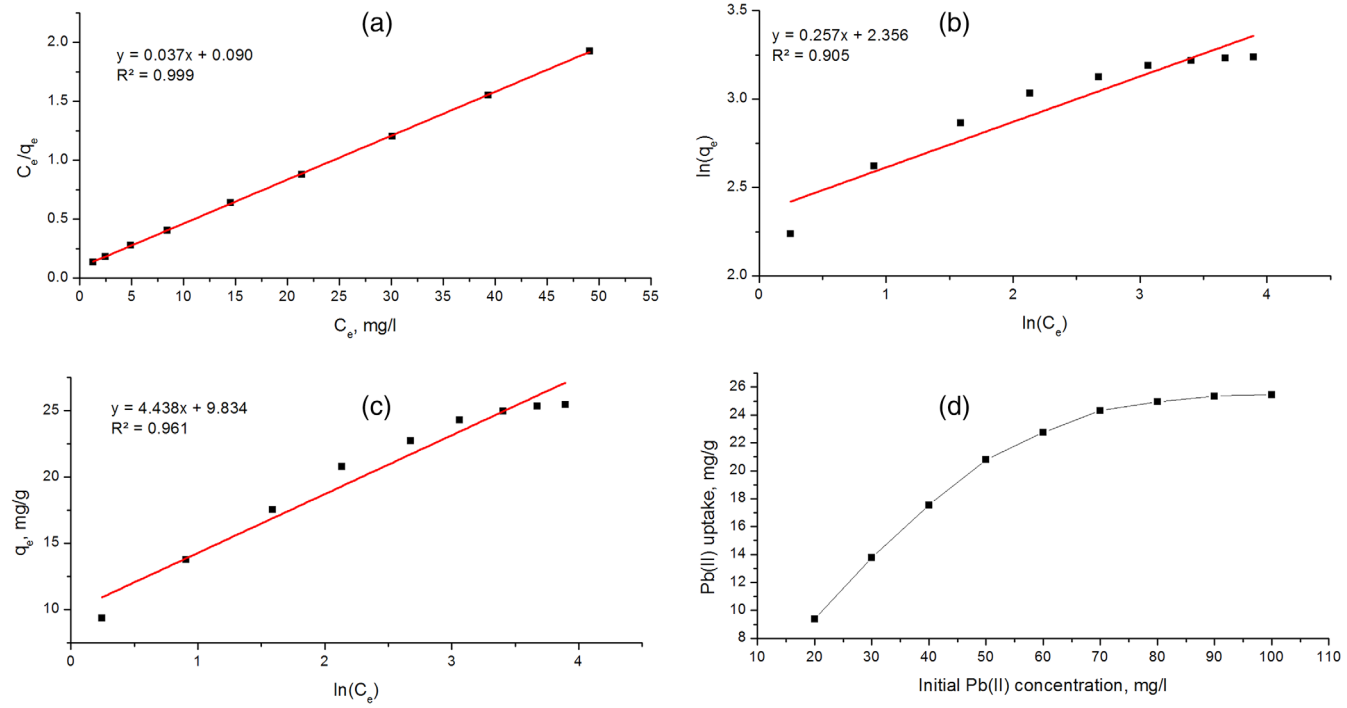

FIGURE 6 Isotherm models for biosorption of Pb(II) (a). Langmuir model (b), Freundlich model (c), and Temkin model (d). Effect of initial concentration on Pb(II) uptake [Color figure can be viewed at wileyonlinelibrary.com]

TABLE 5 Isotherm models for biosorption of Pb(II)

1	Langmuir model $\frac{C_e}{q_e} = \frac{1}{K_L q_{max}} + \frac{C_e}{q_{max}}$	q_{max} (mg g^{-1})	27.02
		K_L (L mg^{-1})	0.411
		R^2	0.999
2	Freundlich model $\ln q_e = \ln K_F + (1/n)\ln C_e$	K_F (mg g^{-1})	1.19
		n mg (g [L $mg^{-1}]^{1/n})^{-1}$	0.42
		R^2	0.905
3	Temkin model $q_e = B\ln A + B\ln C_e$	A (L g^{-1})	4.62
		B (J mol^{-1})	4.438
		R^2	0.961

TABLE 6 Comparison of Pb(II) biosorption capacity of spent *G. acerosa* with other biosorbents

Biosorbent	Capacity (mg g^{-1})	References
Olive cake	19.53	[46]
Calcite	19.92	[47]
Ethylenediamine modified green seaweed (*Caulerpa serrulata*)	2.2	[48]
Jania rubens	29	[49]
Pterocladia capillacea	33.15	[49]
Pinus sylvesteris	22.2	[50]
Spent. *G. acerosa*	27.02	Present study

demonstrated that with the increase of concentration the slope of the plots increased and also found that the breakthrough time is faster. This phenomenon can be ascertained with an increase in

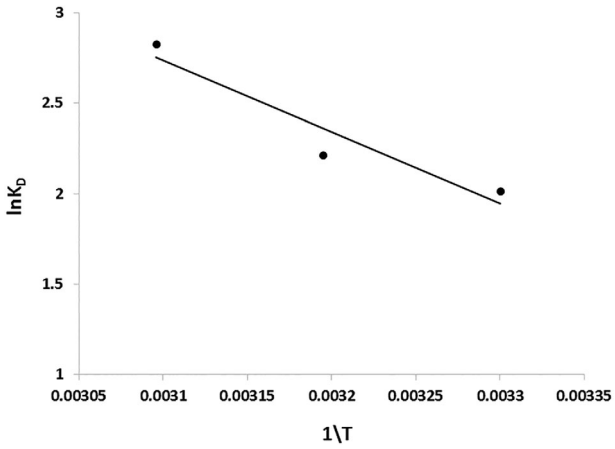

FIGURE 7 Plot of ln(KD) vs 1/*T* for the estimation of thermodynamic parameters

concentration gradient accelerated transfer rate of metal ions onto biosorbent. This increased mass transfer rates enhances the metal binding to biosorbent thereby decreasing bed saturation time hence forth decreased breakthrough time. The same result was reported by Morosanu et al.[52] for Pb(II) biosorption using other biomass. The dynamic parameters obtained from experimental measurements for both inlet concentrations were shown in Table 8. The saturation time was taken as time to reach 90% of inlet concentration whereas breakthrough time was taken as time to reach 10% of inlet concentration. The metal uptake potentials for Pb(II) inlet concentrations of 50 and 100 mg L^{-1} are 43.8 and 71.5 mg g^{-1}, respectively.

TABLE 7 Thermodynamic parameters for biosorption of Pb(II) onto *G. acerosa*

S. No.	T (K)	ΔG^0 (kJ mol^{-1})	ΔH^0 (kJ mol^{-1})	ΔS^0 (J mol^{-1})
1	303	−5.07	32.84	124.79
2	313	−5.76		
3	323	−7.59		

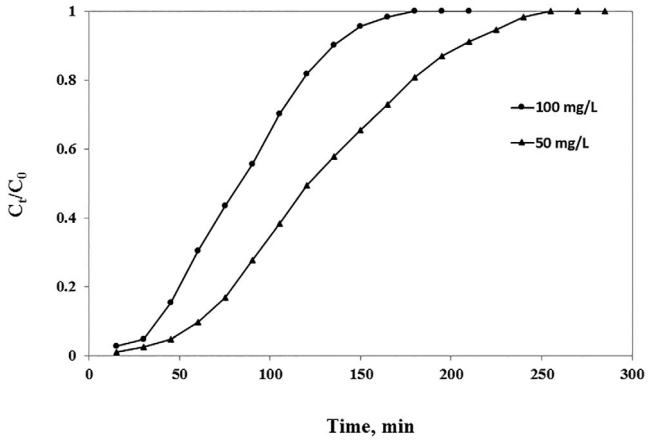

FIGURE 8 Breakthrough plots of fixed bed studies

TABLE 8 Dynamic parameters from breakthrough curves

	Inlet concentration	
Parameter	50 mg L^{-1}	100 mg L^{-1}
t_b (min)	59.84	36.58
t_s (min)	205.10	135.13
q_t (mg g^{-1})	43.8	71.5

3.2.2 | Thomas and Yoon-Nelson parameters

The two prominently employed theoretical models for the assessment of fixed bed column studies such as Thomas and Yoon-Nelson models were used for analysis of column studies data.

Thomas model is the combination of Langmuir isotherm and second order kinetic models[53] and is represented as:

$$\ln\left(\frac{C_0}{C_t}-1\right)=\frac{k_{TH}Q_0W}{F}-k_{TH}C_0t \tag{11}$$

where, k_{TH} is Thomas rate constant, Q_0 is maximum adsorption potential and W is the weight of biosorbent in bed. C_0 and C_t are inlet and outlet metal concentrations. k_{TH} and Q_0 were determined from the slope and intercepts of plot of $\ln(C_0/C_t - 1)$ vs t showed in Figure 9(a). The measured process parameters were summarized in Table 9. The regression coefficients (0.982 and 0.99) of two plots, ie, two concentrations 50 and 100 mg L^{-1} revealing that the experimental findings are well correlated to Thomas model. As shown in Table 9, the constant k_{TH} is decreased and Q_0 is increased with the increase of Pb(II) concentration. The present findings are in good correlation with the results reported by Basu et al.[54]

The Yoon-Nelson model is mainly based on hypothesis of probability of each sorbate molecule adsorption rate decrease is directly proportional to the probability of sorbate breakthrough on the sorbent and the probability of sorbate adsorption.[55] The mathematical expression for this model is:

$$\ln\left(\frac{C_t}{C_0-C_t}\right)=k_{YN}t-k_{YN}\tau \tag{12}$$

where, k_{YN} is Yoon-Nelson constant (L/min) and τ is time of 50% adsorbate breakthrough (min). k_{YN} and τ were calculated from the

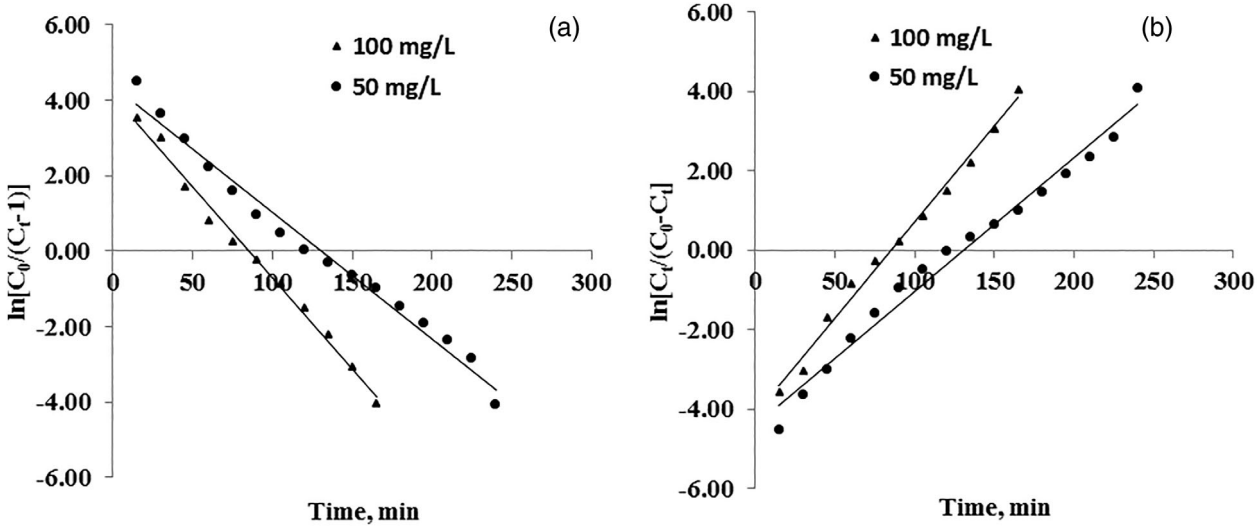

FIGURE 9 (a) Thomas and (b) Yoon Nelson models for biosorption of Pb(II)

TABLE 9 Kinetic models for column studies of biosorption of Pb(II)

S. No.	Model	Constants	Inlet concentration	
			50 mg L^{-1}	100 mg L^{-1}
1	Thomas model	Q_0 (mg g^{-1})	27.859	71.52
		K_{TH} (ml [mg min]$^{-1}$)	0.006	0.0048
		R^2	0.982	0.99
2	Yoon-Nelson model	K_{YN} (L/min^{-1})	0.33	0.48
		τ (min)	133.72	85.91
		R^2	0.982	0.099

slope and intercepts of plot of $\ln(C_t/(C_0 - C_t)$ vs t showed in Figure 9 (b). The results shown in Table 9, reveals that the values of k_{YN} increased from 0.33 to 0.48 min^{-1} with increase of inlet concentration. The regression coefficients 0.982 and 0.99 for 50 and 100 mg L^{-1}, respectively, suggest that the experimental data was good fit to the model. The dynamic biosorption potential obtained from Thomas model for initial Pb(II) concentration of 50 mg L^{-1} is slightly higher than the maximum biosorption potential estimated from Langmuir. Hence, the results demonstrates that continuous mode is preferable than batch mode for biosorption of Pb(II) onto spent *G. acerosa*.

3.3 | Regeneration of biosorbent

Reuse of spent biosorbent is one of the important commercial aspects biosorption. The best approach for regeneration of biosorbent is treatment of spent biosorbent with dilute acid. Hence, Nitric acid has been used as eluent for Pb(II) desorption in batch processes and results showed that the desorption efficiency was 93.5% for first cycle.[7] In addition, the loss of the adsorption capacity of approximately 10% was noticed after the first adsorption–desorption cycle. This parameter remained nearly constant for all the other cycles. Hence, spent *G. acerosa* may be regenerated for many times without a total loss of their biosorption efficiency.

3.4 | Biosorbent characterization

The FT-IR spectra of spent *G. acerosa* (Figure 10) showed several peaks in the range of 4000 to 400 cm^{-1} which indicates the surface of spent biomass of *G.aceroas* is having substantial number of functional groups to capture the metal ions. The broad band at 3319 cm^{-1} indicates N–H stretching, which represents primary amine or O–H alcohol functional groups. The broad peaks noticed at 3003 and 2899 cm^{-1} are associated with C–H bonds of carboxylic groups.[56,57] The major functional groups of cell wall of brown algae are carboxylic and amino groups, which are key elements in metal binding.[58] The sharp peaks in the range of 2157 to 2024 are indicative of C ≡ C stretch, which is associated with alkyne groups. The medium and vibrational peaks in the region of 1721 to 1428 cm^{-1} are the representatives of C=C stretch and are indicatives of multiple bonds of carboxyl groups.[59] Strong stretching vibrations in the

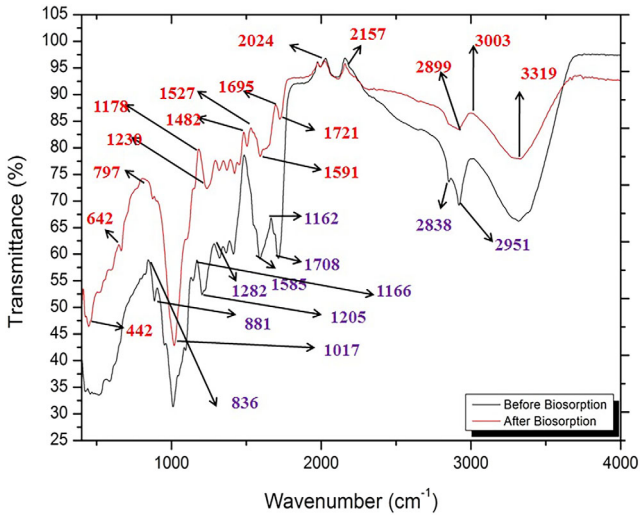

FIGURE 10 FTIR spectrum of biosorption of Pb(II) [Color figure can be viewed at wileyonlinelibrary.com]

range of 1178 to 1071 cm^{-1} are indications of C–O bonds that are associated with the presence of alcohols and phenols. While the broad band at 797 cm^{-1} represents O–H group indicating the strong halide stretch. Therefore the afore mentioned observations are strong indicatives of various functional groups present on the surface of spent *G. acerosa* which plays key role in metal uptake from aqueous solutions.

The spectrum of spent *G. acerosa* loaded with Pb(II) showed (Figure 10) significant changes. The new sharp peaks observed at 2951 and 2838 cm^{-1} and shuffling of peaks from the range of 1721-1482 to 1708-1585 are the clear manifestations of binding of Pb(II) ions to amine and carboxylic groups of spent *G. acerosa*. Further, formation of peaks at 1282 and 1208 are indicating the involvement of C–O group in metal uptake. Moreover, new peaks at 881 and 836 cm^{-1} discloses the binding of Pb(II) ions with C=H group, alkene functional group on the surface of spent *G. acerosa*. Hence, all these observations together demonstrate the attachment of Pb(II) ions with the notable surface functional groups of spent *G. acerosa*.

The SEM monograph of spent *G. acerosa* was recorded to detect the surface texture before biosorption and its modification due to the interactions with loaded Pb(II) ions. The result obtained was illustrated in Figure 11. The spent *G. acerosa* shows very rough surface texture with pores (Figure 11(a)) before biosorption. Hence, there is a great possibility for biosorption of Pb(II) ions onto spent *G. acerosa*. The

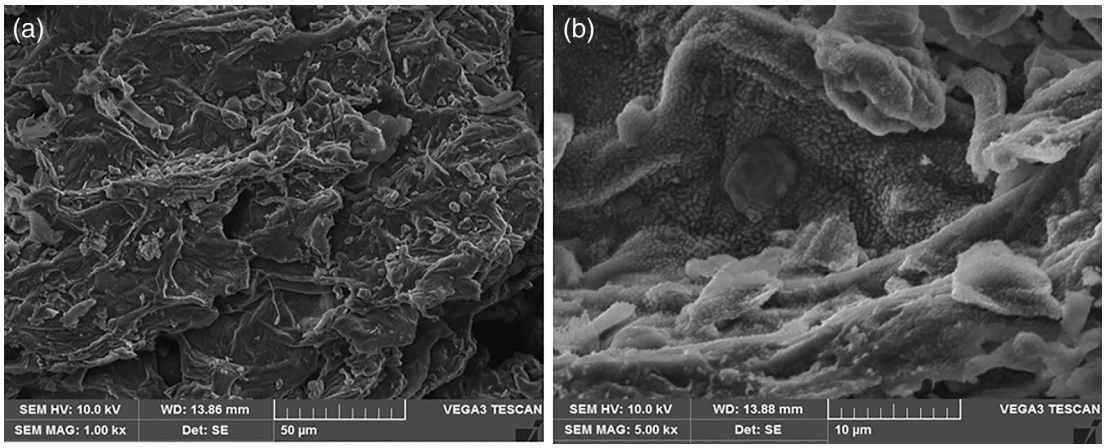

FIGURE 11 SEM images of spent *G. acerosa (a). Before biosorption (b). After biosorption*

smooth surface with closed pores and change of surface color after biosorption as shown in Figure 11(b) signifies the trapping of Pb(II) ions by the surface functional groups.

4 | CONCLUSIONS

The present research was carried out to investigate the lead biosorpton potential of spent *G. acerosa* in batch and fixed bed continuous modes of operation. RSM was used for process optimization and found that initial pH of Pb(II) is the most dominant parameter followed by biosorbent dosage and initial Pb(II) concentration. The maximum Pb(II) removal obtained by RSM is 90.75% at optimum process parameters of initial pH of Pb(II) solution 5.15, initial Pb(II) concentration of 37.35 mg L^{-1} and biosorbent dosage of 0.04 g. Kinetic studies demonstrated that the mechanism behind metal binding is chemical reaction between metal cations and surface functional groups with ion exchange. Further the metal ions transfer rate was controlled by both film diffusion and intra-particle diffusion. Langmuir isotherm showed that the best fit to equilibrium experimental measurements and the maximum lead uptake estimated using this isotherm is 27.02 mg g^{-1}. Fixed bed column studies revealed that metal uptake capacity increased with metal ions concentration in inlet solution. Moreover, the breakthrough times significantly decreased with increase in concentration. Above all concludes that the spent *G. acerosa* could be a successful biosorbent for elimination of lead from industrial effluents. Designing of fixed bed column with spent *G. acerosa* suggests that spent *G. acerosa* can be used as a biosorbent for larger scale industrial operations.

ACKNOWLEDGMENT

I would like to thank entire team of Center of Excellence for Advanced Materials, Manufacturing, Processing and Characterization (CoExAMMPC) of Vignan's Foundation for Science and Technology, Guntur, India.

CONFLICT OF INTEREST

The author declares no conflict of interest.

DATA AVAILABILITY STATEMENT

The author confirms that the data supporting the findings of this study are available within the article and also from the corresponding author upon reasonable request.

ORCID

John Babu D https://orcid.org/0000-0003-4641-915X

REFERENCES

1. Lin D, Ji R, Wang D, et al. The research progress in mechanism and influence of biosorption between lactic acid bacteria and Pb (II): a review. *Crit. Rev. Food Sci. Nutr*. 2019;59:395-410. https://doi.org/10.1080/10408398.2017.1374241.
2. Saini S, Gill JK, Kaur J, et al. Biosorption as environmentally friendly technique for heavy metal removal from wastewater. *Fresh Water Pollution Dynamics and Remediation*. Singapore: Springer; 2020:167-181. https://doi.org/10.1007/978-981-13-8277-2_10.
3. Huang D, Zeng G, Xu P, et al. Biosorption behavior of immobilized *Phanerochaete chrysosporium* for heavy metals removal. *Environ. Eng. Manag. J*. 2018;17:2789-2794.
4. Rahman Z, Thomas L, Singh VP. Biosorption of heavy metals by a lead (Pb) resistant bacterium, *Staphylococcus hominis* strain AMB-2. *J. Basic Microbiol*. 2019;59:477-486. https://doi.org/10.1002/jobm.201900024.
5. Jaishankar M, Tseten T, Anbalagan N, Mathew BB, Beeregowda KN. Toxicity, mechanism and health effects of some heavy metals. *Interdiscip Toxicol*. 2014;7:60-72. https://doi.org/10.2478/intox-2014-0009.
6. Zhang T, Xu W, Lin X, Yan H, Ma M, He Z. Assessment of heavy metals pollution of soybean grains in North Anhui of China. *Sci. Total Environ*. 2019;646:914-922. https://doi.org/10.1016/j.scitotenv.2018.07.335.
7. Basu M, Guha AK, Ray L. Biosorptive removal of lead by lentil husk. *J Environ Chem Eng*. 2015;3:1088-1095. https://doi.org/10.1016/j.jece.2015.04.024.
8. Ara A, Usmani JA. Lead toxicity: a review. *Interdiscip Toxicol*. 2015;8(2):55-64. https://doi.org/10.1515/intox-2015-0009.
9. Malar S, Vikram SS, Favas PJ, Perumal V. Lead heavy metal toxicity induced changes on growth and antioxidative enzymes level in water hyacinths (*Eichhornia crassipes* [Mart.]). *Bot Stud*. 2016;55:54-65. https://doi.org/10.1186/s40529-014-0054-6.
10. Nemati M, Hosseini S, Shabanian M. Novel electrodialysis cation exchange membrane prepared by 2-acrylamido-2-methylpropane sulfonic acid; heavy metal ions removal. *J. Hazard. Mater*. 2017;337:90-104. https://doi.org/10.1016/j.jhazmat.2017.04.074.

11. Barros A, da Silva SKM. Assessment of kinetics, equilibrium and thermodynamics of black krom kjr dye adsorption onto aquatic macrophyte pistia stratiot. *Environ Eng Manag J*. 2018;17:2587-2595.
12. Wierzba S. Biosorption of nickel(II) and zinc(II) from aqueous solutions by the biomass of yeast *Yarrowia lipolytica*. *Pol. J. Chem. Technol*. 2017;19(1):1-10. https://doi.org/10.1515/pjct-2017-0001.
13. Qin H, Hu T, Zhai Y, Lu N, Aliyeva J. The improved methods of heavy metals removal by biosorbents: a review. *Environ. Pollut*. 2019;258: 113777. https://doi.org/10.1016/j.envpol.2019.113777.
14. Chu WL, Phang SM. Biosorption of heavy metals and dyes from industrial effluents by microalgae. In: Alam M, Wang Z, eds. *Microalgae Biotechnology for Development of Biofuel and Wastewater Treatment*. Singapore: Springer; 2019. https://doi.org/10.1007/978-981-13-2264-8_23.
15. Kyzas GZ, Bomis G, Kosheleva RI, et al. Nanobubbles effect on heavy metal ions adsorption by activated carbon. *Chem. Eng. J*. 2019;356: 91. https://doi.org/10.1016/j.cej.2018.09.019.
16. Wang N, Qiu Y, Xiao T, et al. Comparative studies on Pb(II) biosorption with three spongy microbe-based biosorbents: high performance, selectivity and application. *J Hazard Mater*. 2019;373: 39-49. https://doi.org/10.1016/j.jhazmat.2019.03.056.
17. Li F, Wang W, Li C, et al. Self-mediated pH changes in culture medium affecting biosorption and biomineralization of Cd2+ by *Bacillus cereus* Cd01. *J. Hazard. Mater*. 2018;358:178-186. https://doi.org/10.1016/j.jhazmat.2018.06.066.
18. Xu X, Li H, Wang Q, Li D, Han X, Yu H. A facile approach for surface alteration of pseudomonas putida I3 by supplying K_2SO_4 into growth medium: enhanced removal of Pb(II) from aqueous solution. *Bioresour Technol*. 2017;232:79-86. https://doi.org/10.1016/j.biortech.2017.02.038.
19. Filote C, Volf I, Santos SCR, Botelho CMS. Bioadsorptive removal of Pb (II) from aqueous solution by the biorefinery waste of *Fucus spiralis*. *Sci. Total Environ*. 2019;648:1201-1209. https://doi.org/10.1016/j.scitotenv.2018.08.210.
20. Keryanti K, Edi Wahyu SM. Determination of optimum condition of Lead (Pb) biosorption using dried biomass microalgae Aphanothece sp. *Period. Polytech. Chem. Eng*. 2021;65(1):116-123. https://doi.org/10.3311/PPch.15773.
21. Kumar KS, Dahms HU, Won EJ, Lee JS, Shin KH. Microalgae: a promising tool for heavy metal remediation. *Ecotox. Environ. Safe*. 2015; 113:329-352. https://doi.org/10.1016/j.ecoenv.2014.12.019.
22. Mata YN, Blazquez ML, Ballester A, Gonzalez F, Munoz JA. Characterization of the biosorption of cadmium, lead and copper with the brown alga *Fucus vesiculosus*. *J. Hazard. Mater*. 2008;158:316-323. https://doi.org/10.1016/j.jhazmat.2008.01.084.
23. Hannachi Y, Hafidh A. Biosorption potential of *Sargassum muticum* algal biomass for methylene blue and lead removal from aqueous medium. *Int. J. Environ. Sci. Technol*. 2020;17(9):3875-3890. https://doi.org/10.1007/s13762-020-02742-9.
24. Dulla JB, Tamana MR, Boddu S, Pulipati K, Srirama K. Biosorption of copper (II) onto spent biomass of *Gelidiella acerosa* (brown marine algae): optimization and kinetic studies. *Appl. Water. Sci*. 2020;10(2): 1-10. https://doi.org/10.1007/s13201-019-1125-3.
25. Eliescu A, Georgescu AA, Nicolescu CM, et al. Biosorption of Pb (II) from aqueous solution using mushroom (Pleurotus ostreatus) biomass and spent mushroom substrate. *Anal. Lett*. 2020;53(14):2292-2319. https://doi.org/10.1080/00032719.2020.1740722.
26. Dinh VP, Le NC, Tuyen LA, Hung NQ, Nguyen VD, Nguyen NT. Insight into adsorption mechanism of lead(II) from aqueous solution by chitosan loaded MnO_2 nanoparticles. *Mater. Chem. Phys*. 2018; 207:294-302. https://doi.org/10.1016/j.matchemphys.2017.12.071.
27. Tran T, Bui Q, Nguyen T, Ho V, Bach LG. Application of response surface methodology to optimize the fabrication of $ZnCl_2$-activated carbon from sugarcane bagasse for the removal of $Cu2^+$. *Water Sci. Technol*. 2017;75:2047-2055. https://doi.org/10.2166/wst.2017.066.
28. Huynha PT, Nguyenb NT, Vana HN, Nguyenc PT, Nguyene TD, Dinhf VP, (2020). Modeling and optimization of biosorption of lead (II) ions from aqueous solution onto pine leaves (Pinus kesiya) using response surface methodology. *Desal. Water. Treat* 2020; 173: 383–393.doi: https://doi.org/10.5004/dwt.2020.24807.
29. Şentürk I, Alzein M. Adsorptive removal of basic blue 41 using pistachio shell adsorbent-performance in batch and column system. *Sustain. Chem. Pharm*. 2020;16:100254. https://doi.org/10.1016/j.scp.2020.100254.
30. Ajmani A, Patra C, Subbiah S, Narayanasamy S. Packed bed column studies of hexavalent chromium adsorption by zinc chloride activated carbon synthesized from Phanera vahlii fruit biomass. *J. Environ. Chem. Eng*. 2020;8(4):103825. https://doi.org/10.1016/j.jece.2020.103825.
31. Vieira MGA, Oisiovici RM, Gimenes ML, Silva MGC. Biosorption of chromium(VI) using a Sargassum sp. packed-bed column. *Bioresour. Technol*. 2008;99:3094-3099. https://doi.org/10.1016/j.biortech.2007.05.071.
32. Gokhale SV, Jyoti KK, Lele SS. Modeling of chromium (VI) biosorption by immobilized Spirulina platensis in packed column. *J. Hazard. Mater*. 2009;170:735-743. https://doi.org/10.1016/j.jhazmat.2009.05.005.
33. Chauhan D, Sankararamakrishnan N. Modeling and evaluation on removal of hexavalent chromium from aqueous systems using fixed bed column. *J. Hazard. Mater*. 2011;185:55-62. https://doi.org/10.1016/j.jhazmat.2010.08.120.
34. Ferro-García MA, Rivera-Utrilla J, Bautista-Toledo I, Moreno-Castilla C. Adsorption of humic substances on activated carbon from aqueous solutions and their effect on the removal of Cr (III) ions. *Langmuir*. 1998;14:1880-1886.
35. Kusmierek K, Swiątkowski A. Removal of chlorophenols from aqueous solutions by sorption onto walnut, pistachio and hazelnut shells. *Pol. J. Chem. Technol*. 2015;17:23-31. https://doi.org/10.1515/pjct-2015-0005.
36. Aydın H, Baysal G. Adsorption of acid dyes in aqueous solutions by shells of bittim (Pistacia khinjuk stocks). *Desalination*. 2006;196:248-259. https://doi.org/10.1016/j.desal.2005.11.025.
37. Regti A, Laamari MR, Stiriba SE, Haddad ME. Removal of basic blue 41 dyes using *Persea americana*-activated carbon prepared by phosphoric acid action. *Int J Ind Chem*. 2017;8:187-195. https://doi.org/10.1007/s40090-016-0090-z.
38. Mousavi SA, Almasi A, Navazeshkha F, Falahi F. Biosorption of lead from aqueous solutions by algae biomass: optimization and modeling. *Desal Water Treat*. 2019;148:229-237. https://doi.org/10.5004/dwt.2019.23788.
39. Babu DJ, King P, Kumar YP. Optimization of Cu (II) biosorption onto sea urchin test using response surface methodology and artificial neural networks. *Int. J. Environ. Sci. Technol*. 2019;16:1885-1896. https://doi.org/10.1007/s13762-018-1747-2.
40. Sadaf S, Bhatti HN. Batch and fixed bed column studies for the removal of Indosol Yellow BG dye by peanut husk. *J. Taiwan Inst. Chem. Eng*. 2014;45:541-553. https://doi.org/10.1016/j.jtice.2013.05.004.
41. Aljeboree AM, Alkaim AF, Al-Dujaili AH. Adsorption isotherm, kinetic modeling and thermodynamics of crystal violet dye on coconut husk-based activated carbon. *Desal. Water. Treat*. 2015;53:3656-3667. https://doi.org/10.1080/19443994.2013.877854.
42. Wen X, Du C, Zeng G, et al. A novel biosorbent prepared by immobilized *Bacillus licheniformis* for lead removal from wastewater. *Chemosphere*. 2018;200:173-179. https://doi.org/10.1016/j.chemosphere.2018.02.078.
43. Wang XS, Chen LF, Li FY, Chen KL, Wan WY. Removal of Cr (VI) with wheat-residue derived black carbon: reaction mechanism and

adsorption performance. *J. Hazard Mater*. 2010;175:816-822. https://doi.org/10.1016/j.jhazmat.2009.10.082.
44. Deniz F, Kepekci RA. Dye biosorption onto pistachio by-product: a green environmental engineering approach. *J. Mol. Liq*. 2016;219:194-200. https://doi.org/10.1016/j.molliq.2016.03.018.
45. Dawood S, Sen TK. Equilibrium, kinetics and mechanism of removal of methyl blue from aqueous solution by adsorption onto pine cone biomass of *Pinus radiata*. *Water Res*. 2012;46:1933-1946. https://doi.org/10.1016/j.watres.2012.01.009.
46. Doyurum S, Celik A. Pb (II) and Cd (II) removal from aqueous solutions by olive cake. *J. Hazard. Mater*. 2006;138:22-28. https://doi.org/10.1016/j.jhazmat.2006.03.071.
47. Yavuz O, Guzel R, Aydin F, Tegin I, Ziyadanogullari R. Removal of cadmium and lead from aqueous solution by calcite. *Pol. J. Environ. Stud*. 2007;16:467.
48. Mwangi IW, Ngila JC. Removal of heavy metals from contaminated water using ethylenediamine-modified green seaweed (*Caulerpa serrulata*). *Phys. Chem. Earth*. 2012;50–52:111-120. https://doi.org/10.1016/j.pce.2012.08.015.
49. Ibrahim WM. Biosorption of heavy metal ions from aqueous solution by red macroalgae. *J. Hazard. Mater*. 2011;192:1827-1835. https://doi.org/10.1016/j.jhazmat.2011.07.019.
50. Costodes VCT, Fauduet H, Porte C, Delacroix A. Removal of Cd (II) and Pb (II) ions, from aqueous solutions, by adsorption onto sawdust of *Pinus sylvestris*. *J. Hazard. Mater*. 2003;105:121-142. https://doi.org/10.1016/j.jhazmat.2003.07.009.
51. Vijayaraghavan K, Yun YS. Utilization of fermentation waste (Corynebacterium glutamicum) for biosorption of reactive black 5 from aqueous solution. *J. Hazard. Mater*. 2007;141(1):45-52. https://doi.org/10.1016/j.jhazmat.2006.06.081.
52. Morosanu I, Teodosiu C, Paduraru C, Ibanescu D, Tofan L. Biosorption of lead ions from aqueous effluents by rapeseed biomass. *N Biotechnol*. 2017;39:110-124. https://doi.org/10.1016/j.nbt.2016.08.002.
53. Thomas HC. Heterogeneous ion exchange in a flowing system. *J Am Chem Soc*. 1944;66:1664-1666. https://doi.org/10.1021/ja01238a017.
54. Basu M, Guha AK, Ray L. Adsorption of lead on lentil husk in fixed bed column bioreactor. *Bioresour Technol*. 2019;283:86-95. https://doi.org/10.1016/j.biortech.2019.02.133.
55. Yoon YH, Nelson JH. A theoretical model for respirator cartridge service life. *Am Ind Hyg Assoc J*. 1984;45:509-516. https://doi.org/10.1080/15298668491400197.
56. Jerold M, Sivasubramanian V. Biosorption of malachite green from aqueous solution using brown marine macro algae Sargassum swartzii. *Desal. Water. Treat*. 2016;57:25288-25300. https://doi.org/10.1080/19443994.2016.1156582.
57. Dulla JB, Sumalatha B, King P, Yekula PK. Investigation on biosorption of Cd (II) onto *Gelidiella acerosa* (brown algae): optimization (using RSM & ANN) and mechanistic studies. *Desal. Water. Treat*. 2018;107:195-206. https://doi.org/10.5004/dwt.2018.22145.
58. Meseguer VF, Ortuño JF, Aguilar MI, et al. Biosorption of cadmium (II) from aqueous solutions by natural and modified non-living leaves of Posidonia oceanic. *Environ Sci Pollut Res*. 2016;23:24032-24046. https://doi.org/10.1007/s11356-016-7625-x.
59. Khan TA, Mukhlif AA, Khan EA, Sharma DK. Isotherm and kinetics modeling of Pb (II) and Cd (II) adsorptive uptake from aqueous solution by chemically modified green algal biomass. *Model. Earth. Syst. Environ*. 2016;2:117. https://doi.org/10.1007/s40808-016-0157-z.

How to cite this article: D JB. Assessment of lead biosorption performance of spent *Gelidiella acerosa* (marine macro algae): Optimization, isotherm, kinetic, and column studies. *Environ Prog Sustainable Energy*. 2021;e13634. https://doi.org/10.1002/ep.13634